Supporting Information

Biocompatible Polyion Complex Micelles Synthesized from Arborescent Polymers

Vo Thu An Nguyen,[†,‡,⧖] Marie-Claire De Pauw-Gillet,[§] Olivier Sandre,[,†,‡] and Mario Gauthier[*,⧖]*

[†]Univ.Bordeaux, LCPO, UMR 5629, F-33600 Pessac, France

[‡]CNRS, Laboratoire de Chimie des Polymères Organiques, UMR 5629, F-33600 Pessac, France

[§]Mammalian Cell Culture Laboratory, GIGA-R, Université de Liège, B-4000 Liège, Belgium

[⧖]Department of Chemistry, University of Waterloo, Waterloo, ON N2L 3G1, Canada

S1. Synthesis of the Double-Hydrophilic Block Copolymers

S1.1. Experimental Section

Materials. Acetone (Sigma-Aldrich, > 99.7%), dichloromethane (Sigma-Aldrich, > 99.5%), ethyl acetate (Sigma-Aldrich, > 99.8%), tetrahydrofuran (THF, Sigma-Aldrich anhydrous, ≥ 99.9%, inhibitor-free), ethanol (Sigma-Aldrich, ACS reagent, 99.8%), triethylamine (Et_3N, Fisher, ≥ 99.0 %), anisole (Alfa Aesar, 99.0%), trifluoroacetic acid (TFA, Sigma-Aldrich, > 99.0%), methyl 2-bromopropionate (Sigma-Aldrich, 98%), and trimethylsilyl chloride (TMS-Cl, Alfa, ≥ 98.0%) were used as received from the suppliers. Milli-Q water (18.2 MΩ·cm) was obtained from a Milli-Q deionized water purification system (PURELAB Classic, ELGA LabWater).

N,*N*,*N*′,*N*″,*N*″-Pentamethyldiethylenetriamine (PMDETA, Sigma-Aldrich, 99%) was purified by distillation under reduced pressure and stored under N_2 at 4°C. Copper(I) bromide (CuBr, Sigma-Aldrich, 98%) was purified by washing twice (for 4 h and 24 h) with glacial acetic acid (Sigma-Aldrich, 99.75%), three times with absolute ethanol (Sigma-Aldrich, ≥ 99.8%), and finally with diethyl ether (Sigma-Aldrich, anhydrous, ≥ 99.0%). The white powder was dried under vacuum overnight and stored under N_2.

tert-Butyl acrylate (*t*BA, Sigma-Aldrich, 98%) was stirred overnight with freshly crushed calcium hydride (CaH_2, Sigma-Aldrich, lumps, reagent grade, 95%), distilled under reduced pressure and stored under N_2 at 4 °C. 2-Hydroxyethyl acrylate (HEA, Sigma-Aldrich, 96%, with 200–650 ppm hydroquinone monomethyl ether as inhibitor) was purified by liquid-liquid extraction to remove diacrylates and acrylic acid impurities before distillation.[1] An aqueous solution of HEA (81 mL, 0.65 mol) in deionized water (27 mL, 25% v/v) was washed 10 times with *n*-hexanes (Sigma-Aldrich, ACS reagent, ≥ 98.5%) and saturated with sodium chloride. The

HEA in the aqueous phase was then extracted with diethyl ether (Sigma-Aldrich, ACS reagent, ≥ 99.0%, 3 × 75 mL). This monomer solution was dried over anhydrous $MgSO_4$ powder (Fisher, Certified) before concentration by rotary evaporation. Hydroquinone (Alfa Aesar, 99.0%, 75 mg, 0.1% w/w) was added as an inhibitor and the purified monomer was stored at –15 °C until distillation under reduced pressure immediately before use.

Synthesis of Poly(*tert*-butyl acrylate) P*t*BA-Br Macroinitiator. An atom-transfer radical polymerization (ATRP) procedure reported by Davis and Matyjaszewski[2] was adapted. Briefly, methyl 2-bromopropionate (0.368 mL, 3.3 mmol, 1 equiv), CuBr (0.252 g, 1.75 mmol, 0.53 equiv), PMDETA (0.363 mL, 1.74 mmol, 0.52 equiv), degassed acetone (5 mL), and *t*BA (20 mL, 140 mmol, 42.4 equiv) were added to an oven-dried round-bottomed flask (rbf) and the reagent mixture was degassed with 3 freeze-pump-thaw cycles. The green mixture was then placed in an oil bath at 60 °C for 2 h 40 min to reach $\bar{X}_n$ = 13, and 5 h 20 min to reach $\bar{X}_n$ = 27. The reactions were stopped by cooling the flask in liquid nitrogen and non-degassed acetone (ca. 10 mL) was added. The solution was passed through a column (10 cm height × 1 cm diameter) of activated neutral alumina (Sigma-Aldrich, Brockmann I grade, 150-mesh size) using ca. 50 mL acetone as eluent. After removal of the organic solvent by rotary evaporation, the polymer was dissolved in a minimum amount of methanol (ca. 10 mL) and further purified by dialysis in a 1,000 MWCO Spectra/Por® 7 regenerated cellulose bag against 1 L of methanol. The solvent was changed thrice within 24 h, and the polymer was collected by removal of the solvent under vacuum.

P*t*BA$_{13}$ ^{1}H NMR ($CDCl_3$, 400 MHz): $\bar{M}_n$ (NMR) = 1660, DP = 13, δ (ppm): 1.06-1.13 (m, 3H), 1.14-1.65 (b, 140H), 1.65-2.02 (b, 6H), 2.01-2.34 (b, 14H), 2.34-2.62 (b, 2H), 3.55-3.65 (s, 3H), 3.98-4.15 (m, 1H); $\bar{M}_n$ (SEC-PS) = 1724, $Đ_{(SEC)} = \bar{M}_w \cdot \bar{M}_n^{-1}$ = 1.05.

P*t*BA$_{27}$ ^{1}H NMR ($CDCl_3$, 400 MHz): $\bar{M}_n$ (NMR) = 3460, DP = 27, δ (ppm): 1.06-1.13 (m, 3H), 1.14-1.65 (b, 283H), 1.65-2.02 (b, 11H), 2.01-2.34 (b, 28H), 2.34-2.62 (b, 2H), 3.55-3.65 (s, 3H), 3.98-4.15 (m, 1H); $\bar{M}_n$ (SEC-PS) = 3524, $Đ_{(SEC)} = \bar{M}_w \cdot \bar{M}_n^{-1}$ = 1.06.

P*t*BA$_{13}$ and P*t*BA$_{27}$ ^{13}C NMR ($CDCl_3$, 100 MHz) δ (ppm): 27.68 (<u>*C*</u>H_2), 28.08 (C-(<u>*C*</u>H_3)$_3$), 41.88 (<u>*C*</u>H_2-CH-Br), 42.34 (<u>*C*</u>H-CH_3), 80.33 (<u>*C*</u>-$(CH_3)_3$), 174.18 (<u>*C*</u>O).

Silylation of 2-Hydroxyethyl Acrylate. A procedure reported by Mühlebach et al.[3] was adapted. The monomer HEA (75 mL, 0.652 mol, 1.0 equiv), dichloromethane (750 mL) and triethylamine (109.5 mL, 0.79 mol, 1.21 equiv) were added in a 2-L rbf and the solution was cooled to 0 °C in an ice bath. Trimethylsilyl chloride (91.5 mL, 0.72 mol, 1.1 equiv) was then added drop-wise, resulting in the formation of a white precipitate (Et_3N·HCl). The solution was stirred in the ice bath overnight and allowed to reach room temperature gradually. The precipitate was removed by suction filtration (Whatman® filter paper, grade 4), the solvent was removed by rotary evaporation, and the liquid residue was filtered once more. The 2-trimethylsilyloxyethyl acrylate (HEATMS) was purified by dissolution in ethyl acetate (300 mL) and washing with water (300 mL) three times. Anhydrous $MgSO_4$ (ca. 5 g) was then added to the solution which was decanted after 15 min, and the solvent was removed under vacuum.

^{1}H NMR ($CDCl_3$, 400 MHz) δ (ppm): 0.07 (s, 9H), 3.69 (t, J = 4.8 Hz, 2H), 4.10 (t, J = 4.8 Hz, 2H), 5.70 (dd, $^3J_{cis}$ = 10.41 Hz, ^2J = 1.21 Hz, 1H), 6.02 (dd, $^3J_{trans}$ = 17.33 Hz, $^3J_{cis}$ = 10.42 Hz, 1H), 6.30 (dd, $^3J_{trans}$ = 17.33 Hz, ^2J = 1.21 Hz, 1H).

^{13}C NMR ($CDCl_3$, 100 MHz) δ (ppm): -0.62 (Si-(<u>*C*</u>H_3)$_3$), 60.55 (<u>*C*</u>H_2-O-$SiMe_3$), 65.60 (<u>*C*</u>H_2-O-CO), 128.24 (<u>*C*</u>H), 130.72 (<u>*C*</u>H_2-CH), 166.01 (<u>*C*</u>O).

Synthesis of Poly(*tert*-butyl acrylate)-*b*-Poly(2-trimethylsilyloxyethyl acrylate) P*t*BA-*b*-P(HEATMS). P*t*BA-*b*-P(HEATMS) was synthesized by ATRP using either P(tBA)$_{13}$-Br ($\bar{M}_n$ =

1660) or P(tBA)$_{27}$-Br ($\bar{M}_n$ = 3460) as macroinitiator. The procedure reported here used P(tBA)$_{27}$-Br. In a 100-mL Schlenk flask were added CuBr (65 mg, 450 µmol, 1 equiv), anisole (10 mL), PMDETA (93 µL, 44.5 mmol, 0.99 equiv), and freshly distilled HEATMS (31.6 mL, 157 mmol, 350 equiv). The reaction mixture was stirred for 5 min before the addition of PtBA-Br (1.555 mg, 450 µmol, 1.0 equiv). The solution was then degassed by three successive freeze-pump-thaw cycles, the flask was filled with N_2, and heated to 85 °C for 4 h 20 min to reach $\bar{X}_n$ = 60, and 19 h to reach $\bar{X}_n$ = 260. The reactions were stopped by submerging the flask in liquid nitrogen, before the addition of acetone (50 mL). The solution was passed through a column (15 cm height × 2 cm diameter) of activated neutral alumina (Aldrich-Sigma, Brockmann I grade, 150 mesh size) using acetone (100 mL) as eluent. After removal of the organic solvent by rotary evaporation, the polymer was dissolved in a minimum amount of methanol (ca. 30 mL) and further purified by dialysis in a 1,000 MWCO Spectra/Por® 7 regenerated cellulose bag against 1 L of methanol. The solvent was changed thrice within 24 h, and the polymer was collected after removal of the solvent under vacuum.

PtBA$_{13}$-b-PHEATMS$_{50}$ ^{1}H NMR ($CDCl_3$, 400 MHz): $\bar{M}_n$(NMR) = 11060, $\bar{X}_{n,PHEATMS}$ = 50, δ (ppm): 0.14 (s, 450H), 1.06-1.13 (m, 3H), 1.14-1.47 (b, 145H), 1.47-1.74 (b, 70H) 1.74-2.02 (s, 32H), 2.16-2.24 (b, 65H), 3.55-3.72 (b, 103H), 3.88-4.28 (b, 100H); $\bar{M}_n$ (SEC-PS) = 11850, $Đ_{(SEC)}$ = $\bar{M}_w \cdot \bar{M}_n^{-1}$ = 1.15.

PtBA$_{13}$-b-PHEATMS$_{150}$ ^{1}H NMR ($CDCl_3$, 400 MHz): $\bar{M}_n$(NMR) = 29860, $\bar{X}_{n,PHEATMS}$ = 150, δ (ppm): 0.14 (s, 1356H), 1.06-1.13 (m, 3H), 1.14-1.47 (b, 145H), 1.47-1.74 (b, 216H) 1.74-2.02 (s, 86H), 2.16-2.24 (b, 167H), 3.55-3.72 (b, 307H), 3.88-4.28 (b, 318H); $\bar{M}_n$ (SEC-PS) = 37620, $Đ_{(SEC)}$ = $\bar{M}_w \cdot \bar{M}_n^{-1}$ = 1.23.

P*t*BA$_{27}$-*b*-PHEATMS$_{56}$ ^{1}H NMR ($CDCl_3$, 400 MHz): $\bar{M}_n$(NMR) = 14730, $\bar{X}_{n,PHEATMS}$ = 56, δ (ppm): 0.14 (s, 506H), 1.06-1.13 (m, 3H), 1.14-1.47 (b, 283H), 1.47-1.74 (b, 93H) 1.74-2.02 (s, 46H), 2.16-2.24 (b, 83H), 3.55-3.72 (b, 115H), 3.88-4.28 (b, 114H); $\bar{M}_n$ (SEC-PS) = 14350, $Đ_{(SEC)}$ = $\bar{M}_w \cdot \bar{M}_n^{-1}$ = 1.08.

P*t*BA$_{27}$-*b*-PHEATMS$_{260}$ ^{1}H NMR ($CDCl_3$, 400 MHz): $\bar{M}_n$(NMR) = 50450, $\bar{X}_{n,PHEATMS}$ = 260, δ (ppm): 0.14 (s, 2306H), 1.06-1.13 (m, 3H), 1.14-1.47 (b, 283H), 1.47-1.74 (b, 348H) 1.74-2.02 (s, 180H), 2.16-2.24 (b, 286H), 3.55-3.72 (b, 552H), 3.88-4.28 (b, 520H$\bar{M}_n$ (SEC-PS) = 65780, $Đ_{(SEC)}$ = $\bar{M}_w \cdot \bar{M}_n^{-1}$ = 1.16.

P*t*BA-*b*-PHEATMS ^{13}C NMR ($CDCl_3$, 100 MHz), δ (ppm): -0.01 (Si-(<u>*C*</u>H$_3$)$_3$), 23.67(<u>*C*</u>H$_3$-CH), 26.10 (C-(<u>*C*</u>H$_3$)$_3$, 39.43 (<u>*C*</u>H$_2$ backbone), 58.49 (<u>*C*</u>H backbone), 64.60 (<u>*C*</u>H$_2$-O), 66.03 (<u>*C*</u>H$_2$-O-SiMe$_3$), 78.38 (<u>*C*</u>H$_2$-O-CO), 173.07 (<u>*C*</u>O).

Hydrolysis of P*t*BA-*b*-PHEATMS. The procedure reported here was applied to P(*t*BA)$_{27}$-*b*-P(HEATMS)$_{260}$ to produce the corresponding PAA$_{27}$-*b*-PHEA$_{260}$. To a mixture of THF (83 mL) and CH_2Cl_2 (83 mL) was added P(*t*BA)$_{27}$-*b*-P(HEATMS)$_{260}$ (16.5 g, 81.9 mmol HEATMS units, 8.5 mmol *t*BA units, ca. 10% v/v). The flask was cooled in an ice-water bath with vigorous stirring and when the polymer was dissolved, H_2O (5 mL) was added to the solution followed by trifluoroacetic acid (TFA, 277 mL, 3.62 mol, 40 equiv) drop-wise. The solution was left to react for 24 h. The solvent was then removed under vacuum and the deprotected polymer was redissolved in ethanol (EtOH, 30 mL). Solvent exchange was performed by dialysis in a 1,000 MWCO Spectra/Por® 7 regenerated cellulose bag against EtOH (2 L) for 24 h, followed by EtOH/H_2O (50/50 v/v, 2 L) for 24 h, and finally against 6 changes of H_2O (5 L) for 72 h. To accelerate the dialysis, the pH of the H_2O used in the last step was maintained at pH 7 by the addition of NaOH solution. The clear solution obtained was collected and stored at 4°C.

PAA_{13}-*b*-$PHEA_{50}$ ^{1}H NMR (DMSO-d_6, 400 MHz) δ (ppm): 1.01-1.11 (b, 3H), 1.37-1.70 (b, 99 H), 1.70-1.89 (b, 32H), 2.01-2.47 (b, 65), 3.49-3.65 (b, 103H), 3.82-4.24 (b, 100H), 4.58-4.88 (b, 131H).

PAA_{13}-*b*-$PHEA_{150}$ ^{1}H NMR (DMSO-d_6, 400 MHz) δ (ppm): 1.00-1.11 (b, 3H), 1.35-1.70 (b, 177H), 1.74-1.91 (b, 68H), 2.01-2.47 (b, 165), 3.49-3.7 (b, 303H), 3.82-4.24 (b, 300 H), 4.58-4.88 (b, 121H).

PAA_{27}-*b*-$PHEA_{56}$ ^{1}H NMR (DMSO-d_6, 400 MHz) δ (ppm): 1.00-1.11 (b, 3H), 1.35-1.70 (b, 134H), 1.74-1.91 (b, 41H), 2.01-2.47 (b, 81H), 3.49-3.7 (b, 116H), 3.82-4.24 (b, 113 H), 4.58-4.88 (b, 46H).

PAA_{27}-*b*-$PHEA_{260}$ ^{1}H NMR (DMSO-d_6, 400 MHz) δ (ppm): 1.00-1.11 (b, 3H), 1.35-1.70 (b, 379H), 1.74-1.91 (b, 104H), 2.01-2.47 (b, 283H), 3.49-3.7 (b, 523H), 3.82-4.24 (b, 521H), 4.58-4.88 (b, 241H).

PAA-*b*-PHEA ^{13}C NMR (DMSO-d_6, 100 MHz), δ (ppm): 34.35 ($\underline{C}H$), 40.08 ($\underline{C}H_2$), 58.79 ($\underline{C}H_2$-O), 65.63 ($\underline{C}H_2$-OH), 174.07 ($\underline{C}O$).

S1.2. Characterization of Double-Hydrophilic Block Copolymers

Characterization of Polymers. Nuclear magnetic resonance (NMR) ^{1}H, ^{13}C and heteronuclear single quantum coherence (HSQC) spectroscopy were performed on a 400 MHz (100 MHz for the ^{13}C experiments) Bruker Avance I NMR spectrometer with a 5 mm BBFO probe. The apparent molar mass dispersity $Đ_{SEC} = \bar{M}_w \cdot \bar{M}_n^{-1}$ of the polymers was determined by size-exclusion chromatography (SEC) analysis on a PL-GPC 50 Plus (Agilent Technologies) instrument with RI and UV detectors and TOSOH TSK gel columns.

Synthesis of Poly(*tert*-butyl acrylate) P*t*BA-Br Macroinitiator. The ^{1}H NMR spectrum of P*t*BA (Figure SI-1a) is dominated by the *tert*-butyl protons at δ 1.14 – 1.65 ppm (*d*). The $\bar{M}_n$ value of the two homopolymers P(*t*BA)$_{13}$ and P(*t*BA)$_{27}$ was determined by integrating the methine protons in the repeat units (δ 2.01–2.34 ppm, *a2*) and in the terminal unit (next to the bromine atom) at 4.00–4.19 ppm (*a1*). The peak area ratios for the methoxy proton (*b*) to (*a1*), and for the methyl group (*e*) to (*a1*) are both in a 3:1 ratio, which confirms the presence of a single ω–bromine group on every polymer chain and makes this material suitable as macroinitiator in the next ATRP reaction to synthesize the desired block copolymers.

Silylation of 2-Hydroxyethyl Acrylate. In our work, the protection of HEA with a trimethylsilyl group was performed to increase the monomer conversion (otherwise limited to < 50 %)[3] and to achieve fast kinetics, while obtaining well-defined block copolymers with a low dispersity.[3] The structure of the protected monomer was confirmed by ^{1}H NMR analysis.

Synthesis of P*t*BA-*b*-P(HEATMS). The ^{1}H NMR spectrum for the copolymer in Figure SI-1b is dominated by the trimethylsilyl protons signal at δ 0.14 ppm (*f*) and the two strong methylene resonances at 3.5–4.5 ppm (*g* and *h*), which confirms the presence of the HEATMS units in the copolymer. The number-average degree of polymerization of the copolymers was determined from the area of the trimethylsilyl protons at δ 0.14 ppm (*f*) and the methyl groups at δ 1.06-1.13 (*e*). Similar calculations using either the methylene group (*g* or *h*) to (*e*) gave the same $\bar{X}_n$ values, despite the overlap of peaks (*b*) and (*h*). The SEC chromatograms for the two homopolymers and four block copolymers, given in Figure SI-2, confirm the low dispersity of the polymers obtained and the molar mass growth in the second polymerization (chain extension) step.

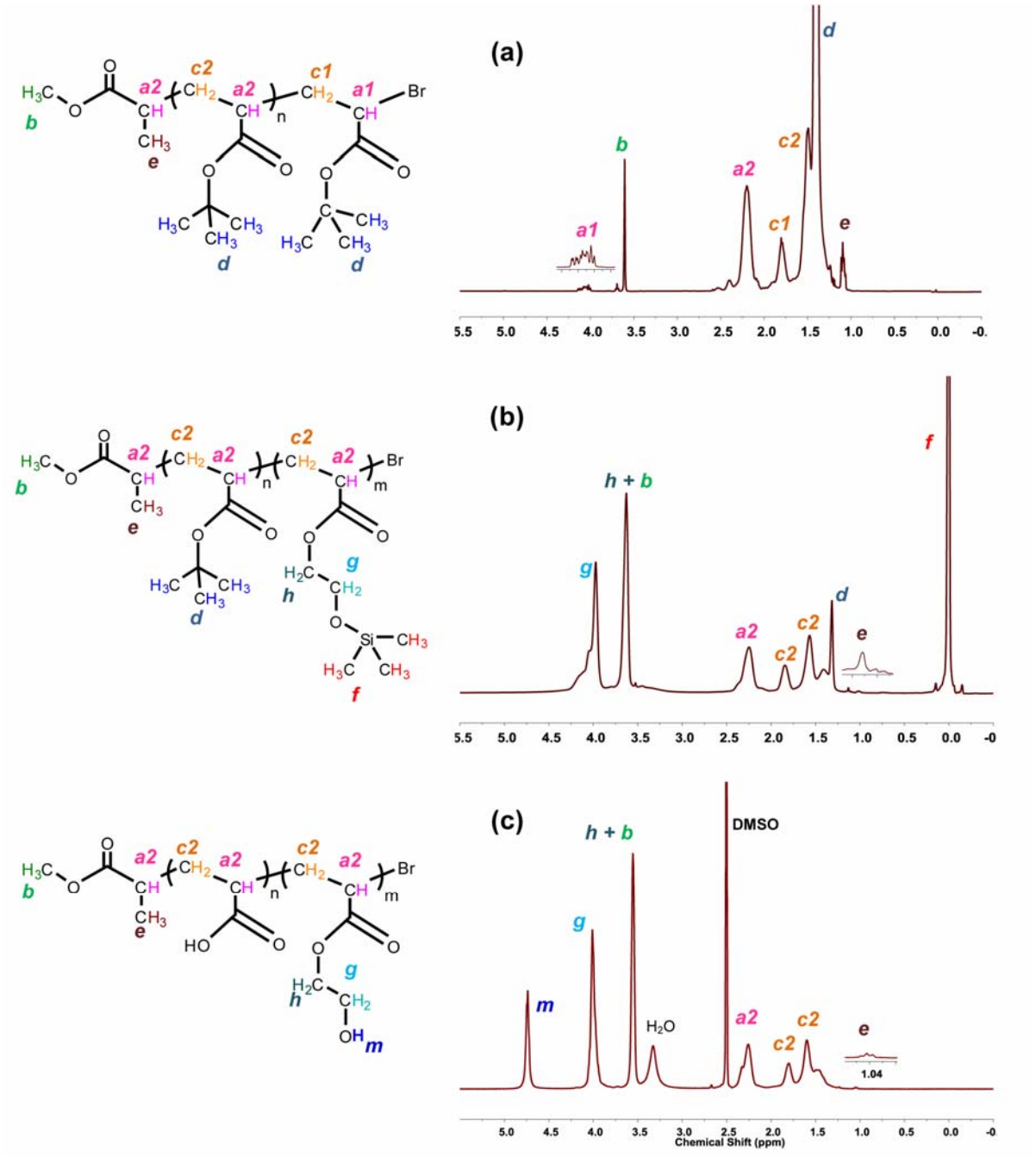

Figure SI-1. ^{1}H NMR (400 MHz) spectra for a) P*t*BA, b) P*t*BA-*b*-P(HEATMS) in $CDCl_3$, and c) PAA-*b*-PHEA in DMSO-d_6.

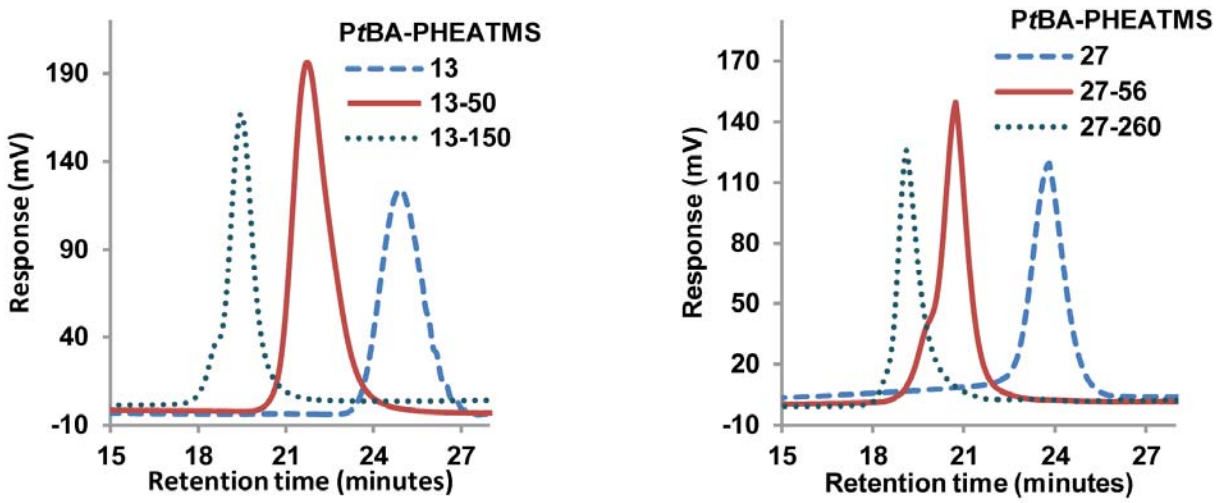

Figure SI-2. SEC chromatograms for P*t*BA homopolymers and P*t*BA-*b*-PHEATMS copolymers.

Hydrolysis of P*t*BA-*b*-PHEATMS. Complete removal of the *tert*-butyl groups was confirmed by *i)* the absence of the peak at δ 1.42 ppm (*d*) in the ^{1}H NMR spectrum (Figure SI-1c), *ii)* the disappearance of the carbon peak at δ 26.10 ppm (*d*) in the ^{13}C NMR spectrum (Section S1.1), and *iii)* the disappearance of the these two resonance signals and their cross-peak in the heteronuclear single quantum coherence spectroscopy (HSQC) NMR spectrum (Figure SI-3). Similarly, complete hydrolysis of the TMS groups was evidenced by *i)* the absence of the resonance at δ 0.14 ppm (*f*), *ii)* the appearance of a hydroxyl proton (*m*) at δ 4.58-4.88 in the ^{1}H NMR spectrum in DMSO-d_6 (Figure SI-1c), *iii)* the disappearance of the carbon peak at δ -0.01 ppm (*f*) in the ^{13}C NMR spectrum (Section S1.1), and *iv)* the disappearance of these two resonance signals and their cross-peaks in the HSQC spectrum (Figure SI-3). The $\bar{X}_n$ of the PHEA segments, calculated by integrating the signals for the methylene group (*g*) and the methyl group (*e*), or for (*h*+*b*) and (*e*), gave the same values. However the $\bar{X}_n$ of the PAA segment could be only calculated by subtraction

of the methine signal for PHEA from the total values for the methine groups (*a2*) of the block copolymer.

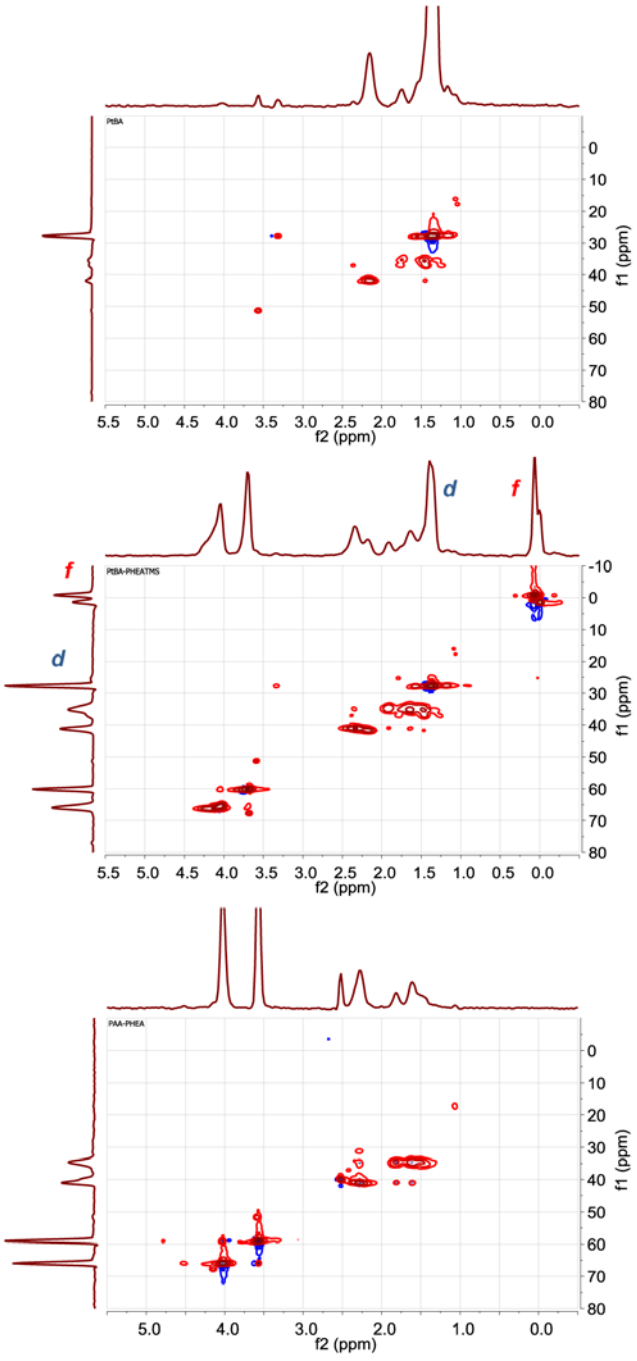

Figure SI-3. HSQC spectra for P*t*BA and P*t*BA-*b*-PHEATMS in $CDCl_3$, and for PAA-*b*-PHEA in DMSO-d_6 (from top to bottom).

S2. Fluorescently Labeled Block Copolymer

S2.1. Experimental Section

The labeled PAA_{27}-*b*-$PHEA_{260}$ copolymer (hereinafter referred to as PAA_{27}^{*}-*b*-$PHEA_{260}$) was prepared via amidation of a small fraction of the carboxylic groups in the PAA block with fluoresceinamine, isomer I (FA, Sigma-Aldrich, 75%), using 1-ethyl-3-(3-dimethylaminopropyl) carbodiimide hydrochloride (EDC, Sigma-Aldrich, ≥ 99.0%) (Scheme SI-1)

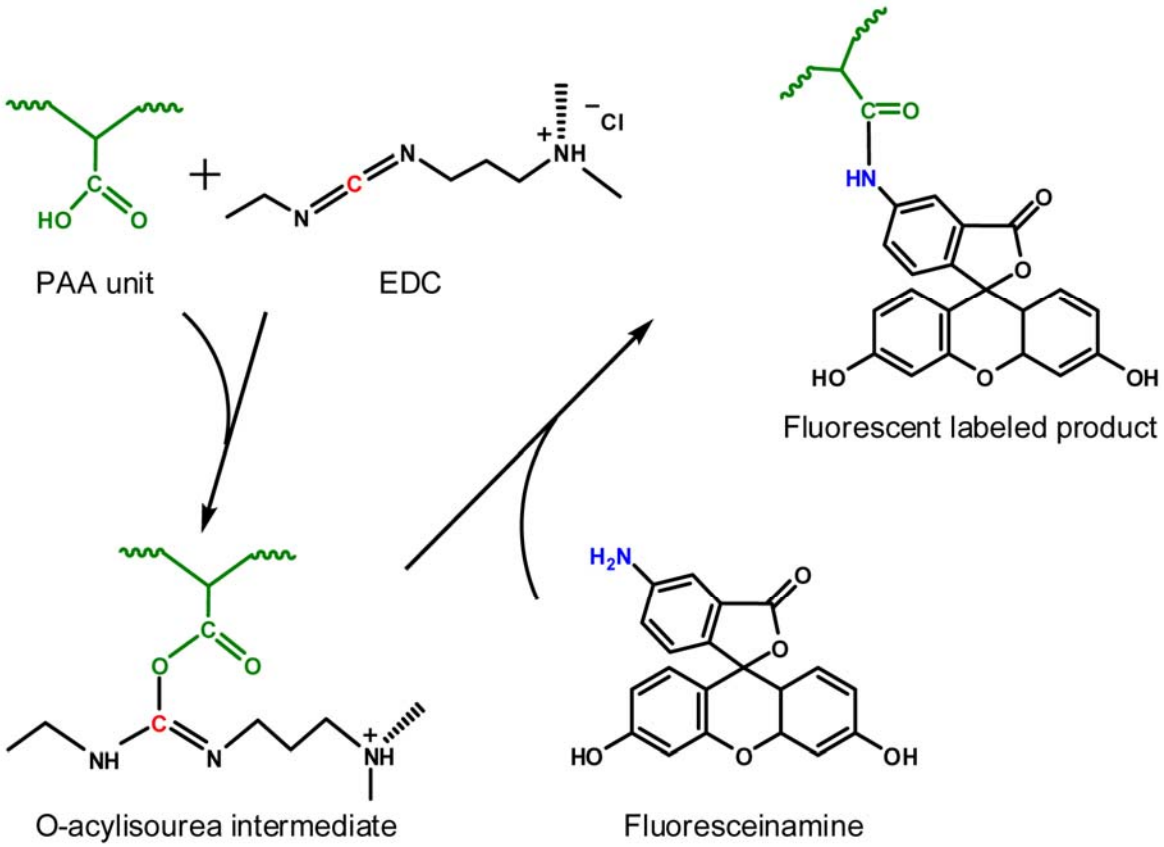

Scheme SI-1. Fluorescent labeling of the PAA units of DHBC PAA-*b*-PHEA mediated by EDC.

A water dispersion of PAA_{27}-*b*-$PHEA_{260}$ (50 mg, 0.162 μmol BC, 43.6 μmol of COOH groups) was prepared while fluoresceinamine (FA, Sigma-Aldrich, 75%, 3.35 mg, 9.65 μmol, FA/COOH = 6/27 mol/mol) was dissolved in DMF (2 mL). The two solutions were combined and vigorously stirred for 10 minutes before 1-ethyl-3-(3-dimethylaminopropyl) carbodiimide hydrochloride (EDC, Sigma-Aldrich, ≥ 99.0%, 67.73 mg, 436 μmol, EDC/COOH = 270/27) was added to create the highly reactive O-acylisourea intermediate. The mixture was allowed to react for 24 h before the product was dialyzed against deionized water for 5 d with 15 changes of water. The PAA_{27}*-*b*-$PHEA_{260}$ copolymer was collected and stored at 10 °C. The fluorescence emission of the block copolymer was monitored on a UV/Vis/Fluorescence SpectraMax® M2e Multimode Microplate Reader.

S2.2. Characterization of Fluorescent Labeled Block Copolymer

An emission band, absent for the non-labeled block copolymer, appeared when PAA_{27}*-*b*-$PHEA_{260}$ was excited at 488 nm (Figure SI-4 Left). A bathochromic shift in the emission peak from 530 nm (for free FA) to 543 nm (for FA conjugated with the block copolymer) was observed, evidencing covalent linking of the dye to the block copolymer. This phenomenon has also been reported for fluorescein isothiocyanate (FITC) and is related to local changes in the environment of the dye (pH, temperature, ionic strength),[4-5] and in particular to polarity (dielectric constant) changes when conjugating FITC with bovine serum albumin (BSA).[6] Therefore the bathochromic shift in the emission peak observed for PIC* micelles (Figure SI-4 Right) indicates the presence of conjugated FA molecules in the micellar structures. To avoid the effects of pH and ionic strength variations, all the samples were prepared in phosphate-buffered saline (PBS) 1× solution (137 mM NaCl, 10 mM K_2HPO_4/KH_2PO_4, 2.7 mM KCl, pH 7.4). A linear relation between the emission

intensity and the concentration of FA in the solution was observed in PBS solution. This correlation curve (Figure SI-4 Middle) was applied to determine the concentration of FA grafted to the block copolymer. The fluorescence emission intensity was recorded at 530 nm for FA in its free form and at 543 nm for PAA*-PHEA. The number of FA molecules conjugated per PAA*$_{27}$-*b*-PHEA$_{260}$ molecule (containing 27 CO_2H groups) determined from the calibration curve was 1.88 ± 0.15, corresponding to 7.0 mol% labeling.

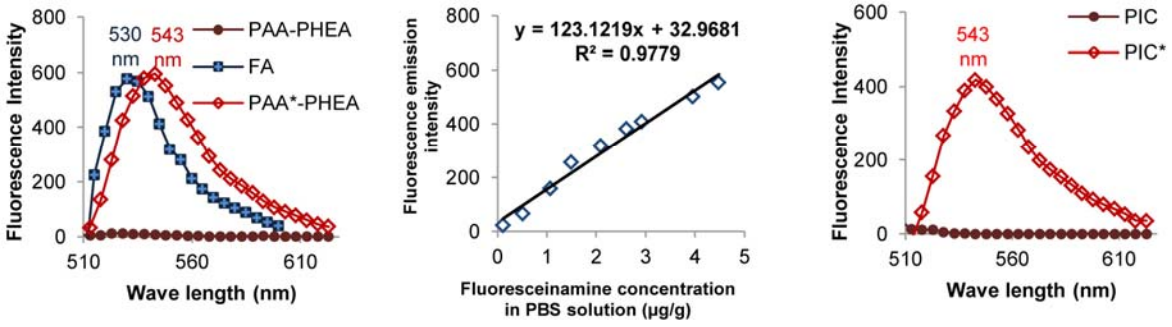

Figure SI-4. (Left) Fluorescence spectra for PAA-*b*-PHEA, free fluoresceinamine and fluorescently labeled PAA*-*b*-PHEA; (Middle) Linear correlation of fluoresceinamine (*Ex*: 488 *Em*: 530) emission intensity vs. concentration in PBS solution and (Right) Fluorescence spectra for PIC and PIC* micelles.

S3. PIC Micelles in Water

S3.1. Preparation of Polyion Complex Micelles.

Complexation of the G1 arborescent copolymer with various amounts of different PAA-*b*-PHEA DHBCs was carried out in aqueous solutions at pH 4.7. The ionization levels of the CO_2H and N functional groups and effective $f^* = CO_2^-/NH^+$ ratios at different pH are shown in Figure SI-5 and Table SI-1.

Hereafter the parameter $f = CO_2H/N$ will be used to quantify the molar ratio between the CO_2H groups (from the PAA segment of the DHBCs) and the N moieties (2VP units of G1). The following procedure describes the complexation of G1 with PAA_{27}-*b*-$PHEA_{260}$ for $f = 0.5$. In a 10-mL vial, G1 (1.7 mg, 14.7 μmol of N) was completely dissolved in 300 μL of aqueous HCl solution at pH 1.4 by sonication (37 kHz, 30 min, Elmasonic™ Ultrasonic Cleaner SH075EL). A pH 7 aqueous solution of PAA_{27}-*b*-$PHEA_{260}$ (8.5 mg, 5 mg·mL^{-1}, 7.35 μmol of CO_2H) was quickly added. The mixture was stirred for 1 h before the pH was adjusted to 4.7 with a 1 M NaOH solution, and stirring was continued for 1 h. The pH was further adjusted to 7 with 0.1 M NaOH and the solution was stirred for 30 min. The solution was then dialyzed (50,000 MWCO Spectra/Por® 7 regenerated cellulose bag) against Milli-Q water (5 L) for 24 h before it was collected and stored at 4 ºC.

pH	CO_2^- / total CO_2H^a	NH^+ /total N^b
1.4	0.00%	99.9%
4.7	1.6%	67%
7	76%	1%

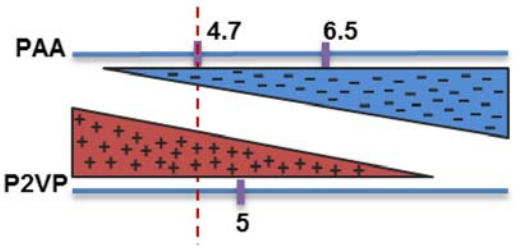

[a] Based on the Henderson–Hasselbalch equation for poly(acrylic acid), $pK_a = 6.5$

$$pH = pK_a + \log\frac{[CO_2^-]}{[CO_2H]}$$

[b] Based on the Henderson–Hasselbalch equation for protonated poly(2-vinyl pyridine), $pK_a = 5$

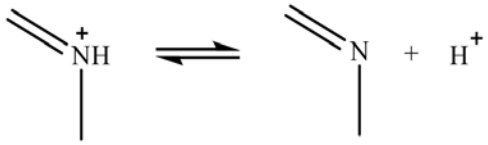

$$pH = pK_a + \log\frac{[N]}{[NH^+]}$$

Figure SI-5. Ionization levels of CO_2H and N functional groups at different pH.

Table SI-1. Effective $f^* = CO_2^-/NH^+$ ratios at pH 4.7 and 7.

f **pH 4.7**	CO_2^- equiv	CO_2H equiv	NH^+ equiv	N equiv	$f^* = CO_2^-/NH^+$
9	0.140	8.860	0.667	0.333	0.211
6	0.094	5.906	0.667	0.333	0.140
3	0.047	2.953	0.667	0.333	0.070
1	0.016	0.984	0.667	0.333	0.023
0.5	0.008	0.492	0.667	0.333	0.012
0.25	0.004	0.246	0.667	0.333	0.006
0.125	0.002	0.123	0.667	0.333	0.003

f **pH 7**	CO_2^- equiv	CO_2H equiv	NH^+ equiv	N equiv	$f^* = CO_2^-/NH^+$
9	6.838	2.162	0.010	0.990	684
6	4.558	1.442	0.010	0.990	456
3	2.279	0.721	0.010	0.990	228
1	0.760	0.240	0.010	0.990	76
0.5	0.380	0.120	0.010	0.990	38
0.25	0.190	0.060	0.010	0.990	19
0.125	0.095	0.030	0.010	0.990	9

S3.1. Single Angle Dynamic Light Scattering and Laser Velocimetry (Zetametry)

The DLS measurements were performed in triplicate using disposable PS cuvettes or quartz cuvettes on a Zetasizer™ Nano ZS90 (Malvern Instruments) equipped with a 4 mW He-Ne laser operating at 633 nm and 25.0 °C, at a scattering angle of 90°. Zeta potential measurements were also performed on the same equipment by the phase analysis light scattering (PALS) method using Malvern DTS1070 folded capillary cells with embedded gold electrodes. The ZP was calculated from the electrophoretic mobility (μ), the dielectric constant (ε) and the viscosity (η) of water using the Schmolukovski equation $\mu = \mathrm{ZP} \times \varepsilon/\eta$. In all cases where an intensity-weighted unimodal size distribution was obtained by DLS analysis, similar results were also obtained for number- and volume-weighted distribution curves, but with the classical shift of the peak positions $D_{\mathrm{h}}^{\mathrm{n}} < D_{\mathrm{h}}^{\mathrm{w}} < D_{\mathrm{h}}^{\mathrm{I}}$, as ascribed to the different weighting methods of the size distribution (Figures SI-6 and SI-7).

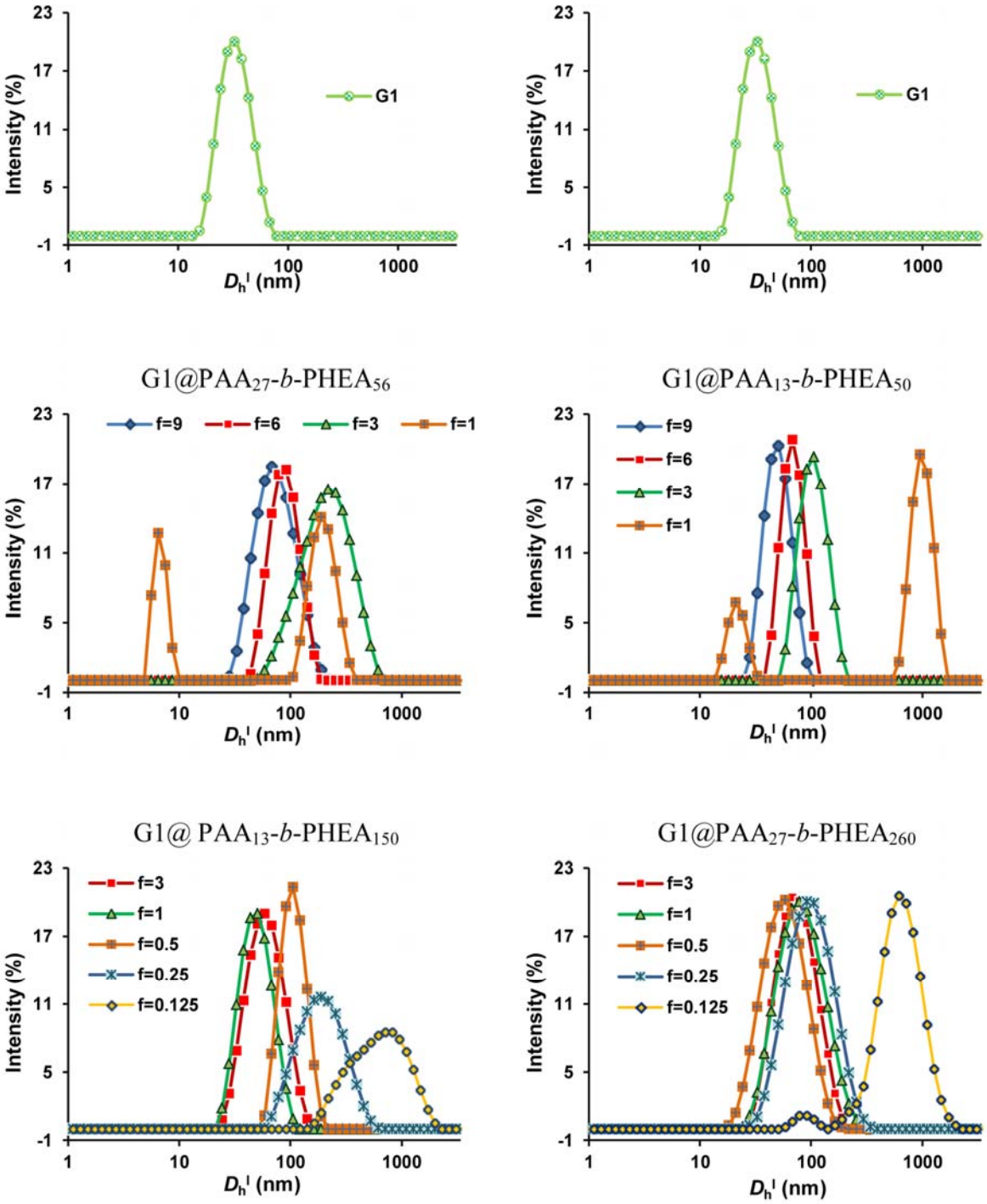

Figure SI-6. Intensity-weighted size distributions for G1 (pH 4) and G1@PAA-*b*-PHEA PIC micelles (pH 7) obtained at various *f* ratios at 25 °C**.**

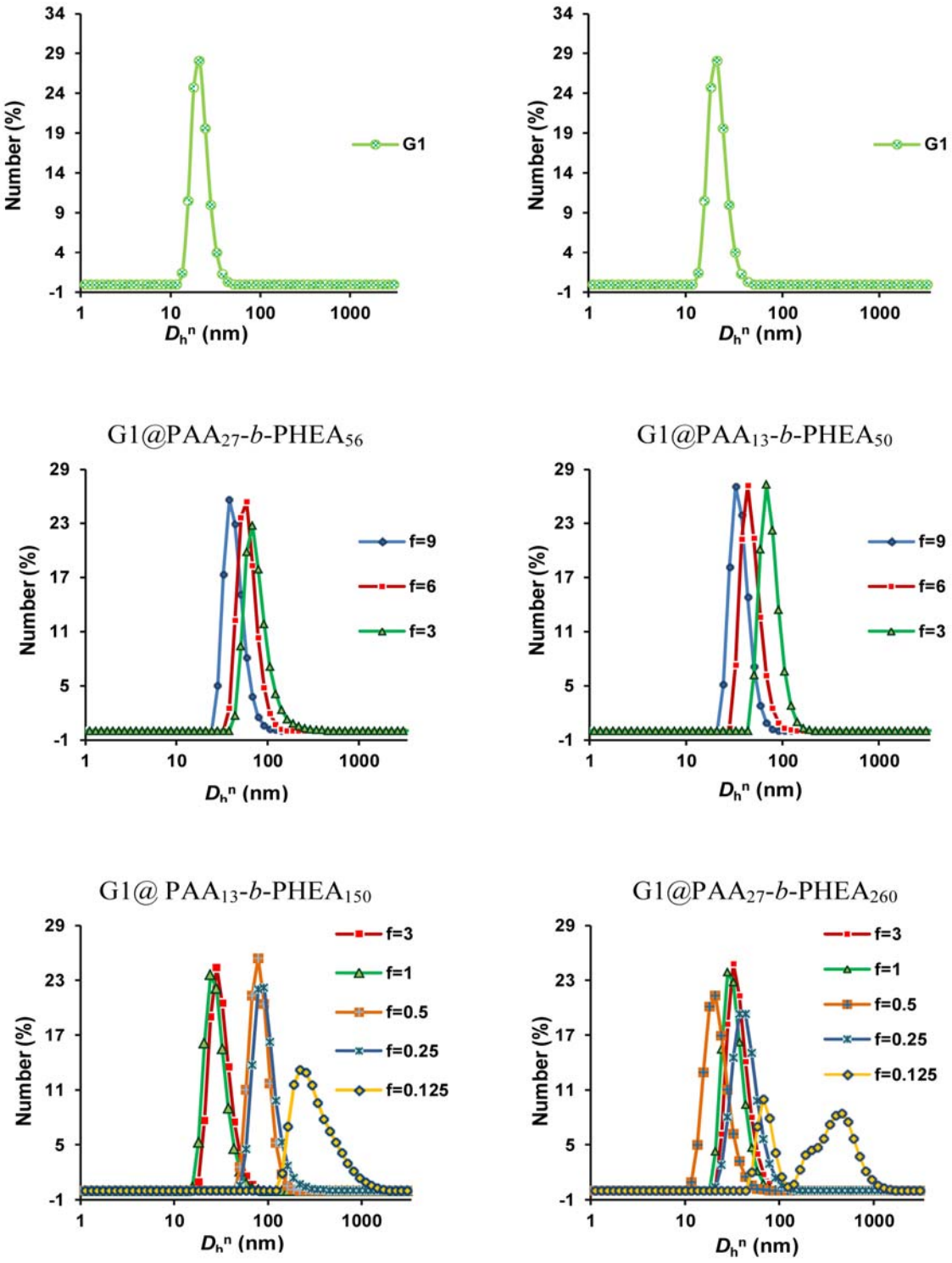

Figure SI-7. Number-weighted size distributions for G1 (pH 4) and G1@PAA-*b*-PHEA PIC micelles (pH 7) obtained at various *f* ratios at 25 °C**.**

S3.2. Refractive Index Increment Determination

For selected PIC systems, the refractive index increment (d*n*/d*c*) was determined using a differential refractometer (Wyatt Technology) at 658 nm, by injecting a series of 5 micellar solutions at 0.2–1 mg·mL^{-1}. The data were processed with the ASTRA 6 software. The linear correlation found between d*n*/d*c* vs. composition was used to interpolate the d*n*/d*c* values for the other PIC systems.

We selected three PIC micelle systems due to their smaller size, to minimize intraparticle scattering effects and to avoid sedimentation of the particles. The d*n*/d*c* values for the PIC micelles (Table SI-2 Top) display consistent trends, with a magnitude increasing with the weight fraction of the higher refractive index components (PS and P2VP) as expected. The correlation coefficients were higher than 0.9999 in all cases. The linear correlation found between d*n*/d*c* vs. composition was used to interpolate the d*n*/d*c* values for the other PIC systems (Table SI-2 Bottom).

Table SI-2. Measured (top) and calculated (bottom) refractive index increments for selected PIC micelles. (Inset) Measured d*n*/d*c* of the PIC micelles as a function of composition

Samples	**G1@PAA$_{13}$-*b*-PHEA$_{150}$**	**G1@PAA$_{27}$-*b*-PHEA$_{260}$**	
f	3	1	0.5
%wt G1	3.3	10.5	16.5
d*n*/d*c* (mL/g)	0.1294 ± 0.0005	0.1367 ± 0.0002	0.1389 ± 0.0004
R^2	0.99993	0.99999	0.99996

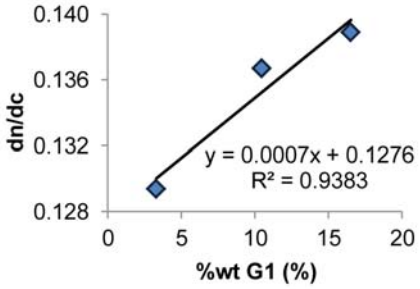

Samples	**G1@PAA$_{13}$-*b*-PHEA$_{150}$**			**G1@PAA$_{27}$-*b*-PHEA$_{260}$**		**G1@PAA$_{13}$-*b*-PHEA$_{50}$**	**G1@PAA$_{27}$-*b*-PHEA$_{56}$**
f	1	0.5	0.25	3	0.25	9	9
%wt G1	7.9	15.3	31.1	3.4	36.8	3.4	5.9
Cal. d*n*/d*c* (mL/g)	0.1334	0.1388	0.1503	0.1301	0.1545	0.1301	0.1319

S3.3. Multi-Angle Static and Dynamic Laser Light Scattering

Light scattering measurements were performed for 5 samples at 0.2–1 mg·mL^{-1} in aqueous solutions at 25°C, at 25 scattering angles θ ranging from 30 to 150°, using an ALV™/CGS-3 platform-based goniometer system equipped with a He-Ne laser (λ = 632.8 nm, 22 mW output power), a proprietary ALV™ optical fiber-based detector, an APD-based single photon detector, ALV™/LSE-5003 Electronics, and an ALV™-5000/EPP correlator. For the static measurements, the intensity of scattered light was measured with the photomultiplier detector and the data were analyzed by the Zimm extrapolation technique to zero concentration and angle. Zimm plots for PIC micelles with G1@PAA-*b*-PHEA for various *f* ratio are shown in Figures SI-8, SI-9 and SI-10.

Multi-angle dynamic light scattering data were also collected at a concentration of 1 mg·mL^{-1}, whereby using the intensity autocorrelation function, the mean decay rate $\langle\Gamma\rangle$ obtained by 2nd order cumulants analysis was plotted *vs.* the square of the wave-vector $q = (4\pi n/\lambda)sin(\theta/2)$. The good linear regression results obtained for the $\langle\Gamma\rangle$ *vs.* q^2 plots with zero intercept was consistent with a low size dispersity. The slope was taken as the translational diffusion coefficient, yielding the multi-angle hydrodynamic radius values R_h reported in Table 2. At each angle, the 2nd order cumulant fitting parameter μ_2 was used to derive the polydispersity index (PDI) through $PDI = \mu_2/\langle\Gamma\rangle^2$. An example of a plot of $\langle\Gamma\rangle$ *vs.* q^2 is given in Figure SI-11. The error bars represent the standard deviation calculated according to the equation $\sqrt{\mu_2} = \langle\Gamma\rangle \cdot \sqrt{PDI}$.[7]

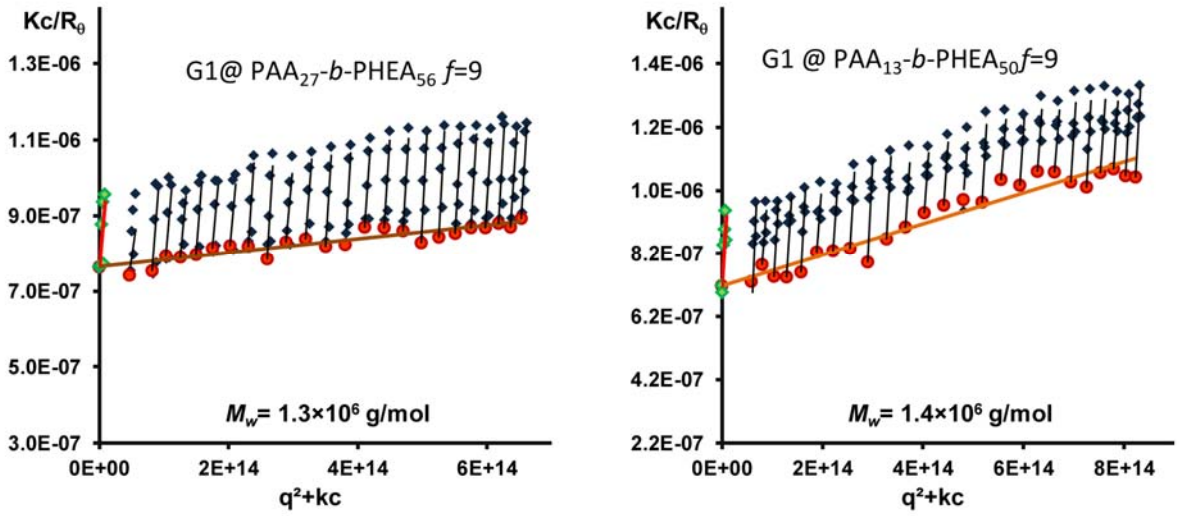

Figure SI-8. Zimm plots for PIC micelles G1@PAA$_{27}$-*b*-PHEA$_{56}$ and G1@PAA$_{13}$-*b*-PHEA$_{50}$ for $f = 9$.

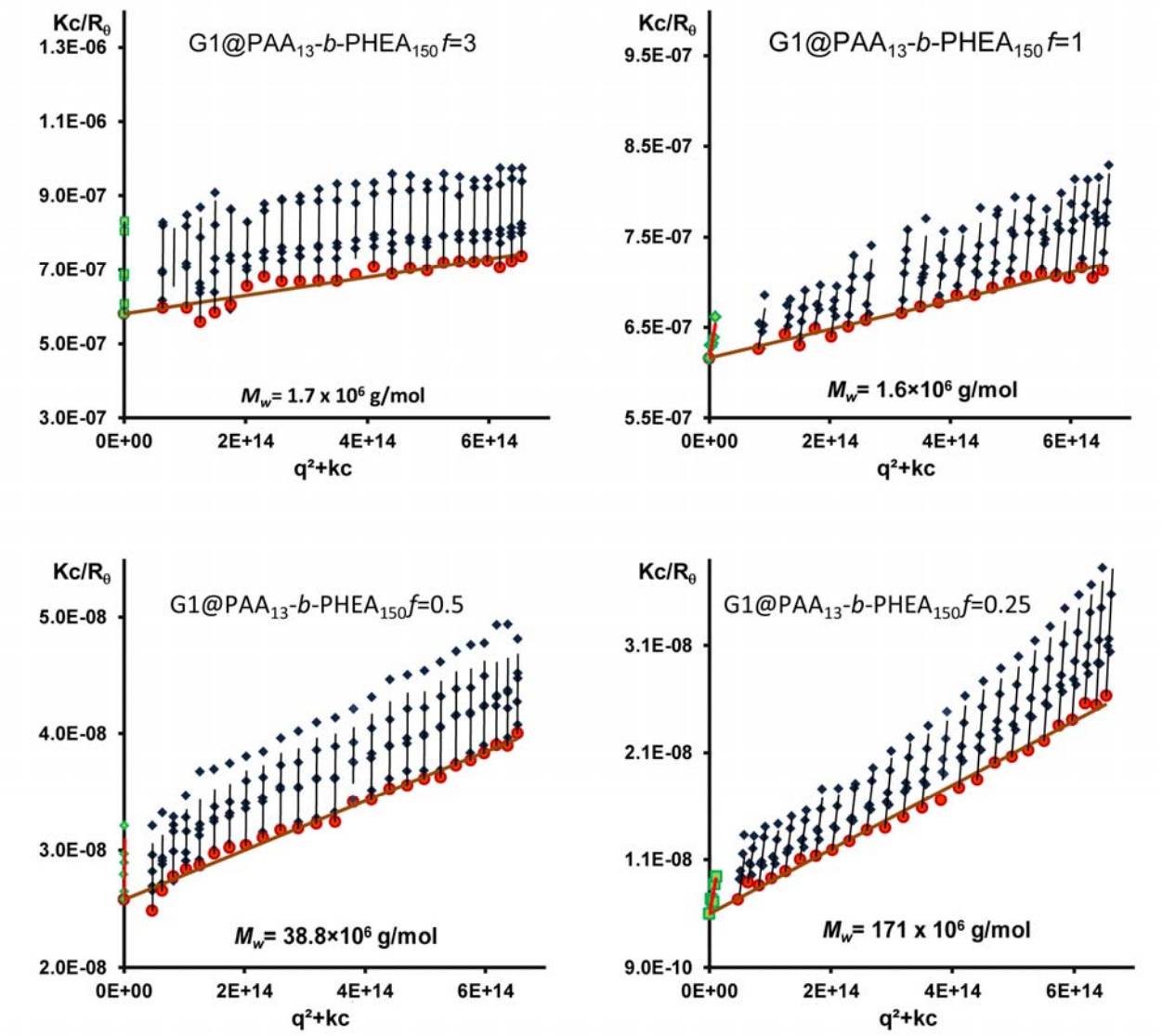

Figure SI-9. Zimm plots for PIC micelles G1@PAA$_{13}$-*b*-PHEA$_{150}$ for different *f* ratios. The red circles indicate extrapolation to zero-concentration (slope giving the radius of gyration R_g), and the green circles, the extrapolation to zero-angle (slope giving the 2nd virial coefficient A_2), while the intercept is the inverse of the weight-average molar mass ($\bar{M}_w$) of the scatterers.

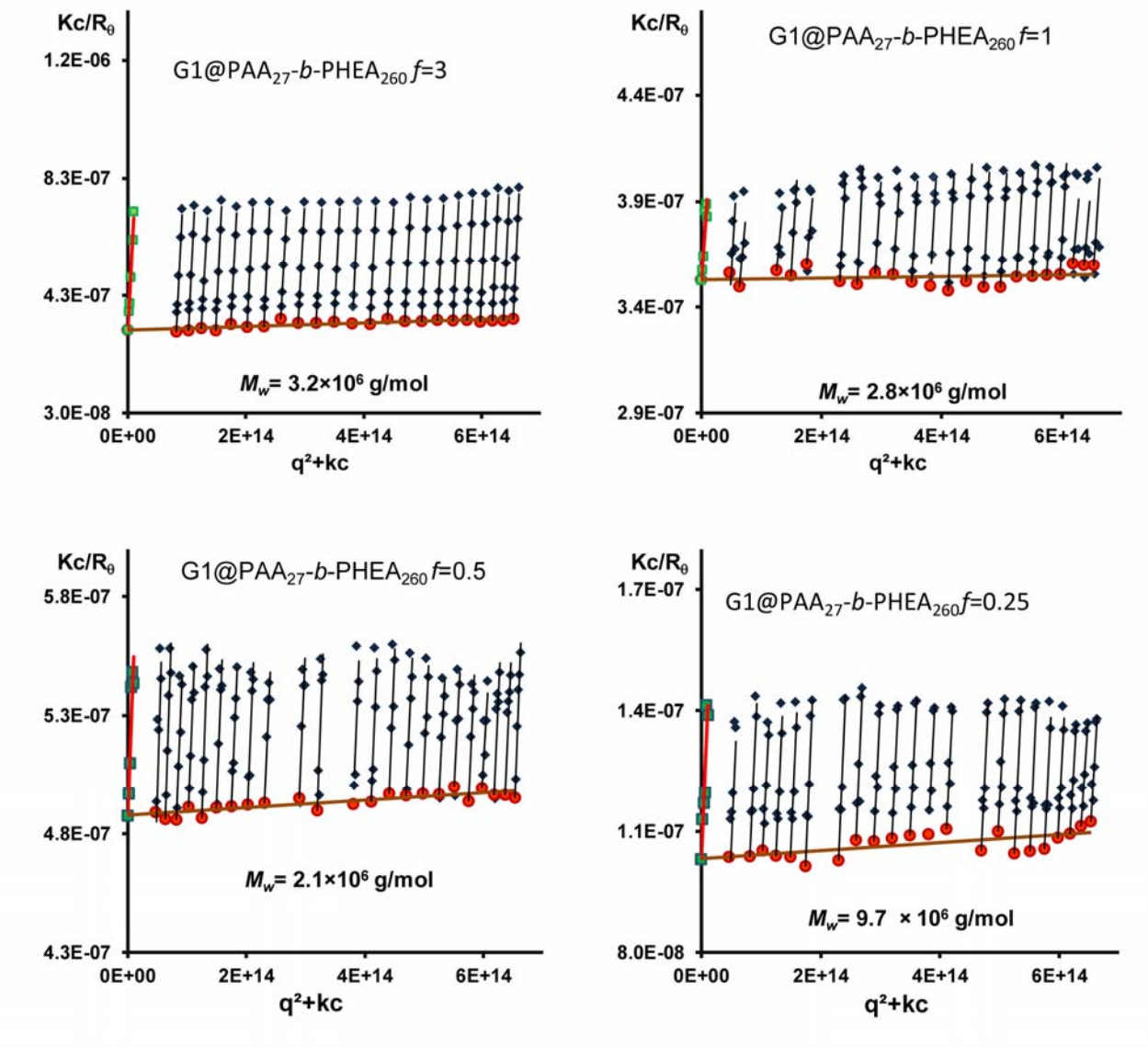

Figure SI-10. Zimm plots for PIC micelles G1@PAA$_{27}$-*b*-PHEA$_{260}$ for different *f* ratios.

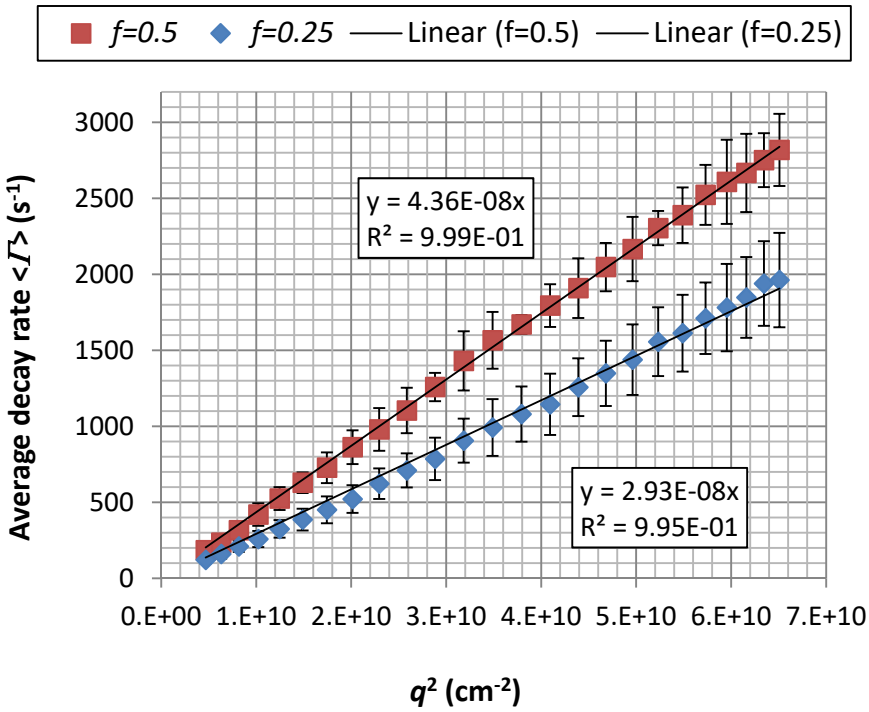

Figure SI-11. Example of multi-angle DLS measurements: G1@PAA$_{13}$-*b*-PHEA$_{150}$ at $f = 0.25$ and $f = 0.5$ and a concentration of 1 mg·mL^{-1}.

S3.4. Atomic Force Microscopy

For Tapping Mode™ atomic force microscopy (AFM), a 20 µL aliquot of PIC dispersion (0.05–0.1 mg·mL^{-1} in water) was deposited on the freshly cleaved mica substrate and spin-coated at 3000 rpm for 180 s under ambient conditions. AFM images were recorded in the tapping mode in air on a Veeco Dimension Icon System equipped with a Nanoscope V controller. The probes used were Olympus® AC160TS-R3 micro cantilevers (spring constant 26–56 N/m, resonance frequency 300–399 kHz, curvature radius 8–10 nm). The scan rate was typically between 0.7 and 1.2 Hz, at a scan angle of 0°, acquiring 512 samples/line.

S4. Biocompatibility Assessment

S4.1. Materials

For the cell cultures, Dulbecco modified Eagle medium (DMEM, with 4.5 $g \cdot L^{-1}$ glucose, sodium bicarbonate, without sodium pyruvate, sterile-filtered, suitable for cell culture), GlutaMAX, fetal bovine serum (FBS), and 0.5% trypsin solution 10× were purchased from Gibco, Grand Island, NY. Sodium pyruvate was obtained from Biowhittaker (Walkersville, MD). PBS solution (with Ca^{2+} and Mg^{2+}), PBS solution (without Ca^{2+} and Mg^{2+}), penicillin and streptomycin were purchased from Lonza. The mouse fibroblast-like L929 cell line was purchased from LifeTechnologies. 3-(4,5-Dimethylthiazol-2-yl)-5-(3-carboxymethoxyphenyl)-2-(4-sulfophenyl)-2H-tetrazolium (MTS) was obtained from Promega (Madison, WI) for the cell viability tests. Paraformaldehyde (Sigma-Aldrich, powder 95%), Triton X-100 (Sigma-Aldrich, BioXtra, for molecular biology), bovine serum albumin (BSA), Alexa Fluor® 594 phalloidin (Life Technologies, 300 units), 4',6'-diamidino-2-phenylindole (DAPI, Sigma-Aldrich 98.0%), and Vectashield HardSet Mounting Medium with DAPI (Vector laboratories) served for the cell internalization experiments.

S4.2. Cell Cultures

The fibroblast-like L929 cells derived from normal subcutaneous areolar and adipose tissue of a 100-day old male C3H/An mouse[8] were purchased from LifeTechnologies™. L929 cells were cultured in DMEM supplemented with 10 vol% of heat-inactivated fetal bovine serum (FBS), 1 vol% of antibiotics (10,000 units of penicillin and 10,000 units of streptomycin/mL), 1 vol% sodium pyruvate and 1 vol% GlutaMAX. The cells were maintained at 37 °C in a 5% CO_2 humidified incubator. After rinsing with PBS (Ca^{2+}/Mg^{2+} free) solution to remove the serum, the cells were detached with trypsin solution 10× diluted 10-fold with PBS (Ca^{2+}/Mg^{2+} free) solution. The PBS solution used contained Ca^{2+}/Mg^{2+} unless otherwise noted (e.g., Ca^{2+}/Mg^{2+} free).

S4.3. Cytotoxicity Assessment

After detachment, the L929 cells were seeded in a 96-well plate at a density of 2×10^3 cells/well, and grown in DMEM complete medium in a humidified incubator (5 vol% CO_2) at 37 °C for 24 h prior to treatment. The PIC micelle solutions with different final concentrations in the culture medium (10, 2, 1, 0.4 and 0.2 mg of PIC micelles/mL) were prepared in a mixture of 10% PBS solution and 90% DMEM complete medium before cell treatment. The cells were exposed to PIC micelle solutions and incubated for 48 h. The medium was removed and the cells were rinsed with PBS solution (100 µL/well). A 120 µL aliquot of MTS solution (containing 20 µL of MTS solution and 100 µL of PBS solution) was then added into each well. The plates were incubated at 37 °C for 120 min. The absorbance at 490 nm was measured on a PowerWave X (BioTek Instrument Inc.) micro-plate UV-VIS spectrometer. The positive controls were cells incubated with a mixture of 10% PBS solution and 90% DMEM complete medium alone. The results were expressed as the percentage of metabolic activity of treated cells relatively to untreated cells (control, 100% viability). Independent experiments were performed 3 times with 4 replicates per condition.

S4.4. Cell Internalization Study by Confocal Laser Scanning Microscopy

The L929 cells were seeded on the surface of a sterile glass coverslip placed in the well of a 12-well plate at a density of 5×10^4 cells/2 mL/well and allowed to attach and to grow at 37 °C in a 5% CO_2 humidified incubator. The fluorescently labeled PIC* micelle solution (2 mg of PIC* micelles/mL) was prepared in a mixture of 10% PBS solution and 90% DMEM complete medium before cell treatment. After 24 h of cell growth the DMEM complete medium was replaced with 2 mL of PIC* micelle suspensions. From this point the plate was protected from light exposure by wrapping in aluminum foil when it was not in use. After 24 h of exposure to the nanoparticles, the suspension was removed and the cells were rinsed twice with PBS solution to completely remove non-taken nanoparticles. The cells were then fixed with 2 mL of paraformaldehyde cross-linking agent (4 vol%) diluted in PBS solution (4 ºC, 20 min). The fixative solution was removed and the cells were washed twice with PBS solution. Permeabilization of the cell membranes was performed by treating the cells with 2 mL of 0.5 vol% Triton X-100 in PBS solution (4 ºC, 20 min). The Triton X-100 solution was removed and the cells were rinsed twice with PBS solution. The protein-binding sites on the membranes were blocked by incubating with 1 vol% BSA in PBS solution (2 mL, 37 ºC, 30 min). The blocking agents were removed and the cells were washed twice with PBS solution before 2 mL of 1.67 vol% of Alexa Fluor® 594 phalloidin in PBS solution was added to label the *F*-actin cytoskeleton of the fixated cells. The actin staining was allowed to occur for 1 h at 37 ºC in the humidified incubator before the cells were washed twice with PBS solution. The cell nuclei were then stained with 2 mL of 0.025 vol% of DAPI in PBS solution (10 min, 4 ºC). The staining solution was removed and the cells were rinsed twice and stored in 0.05 vol% of Tween-20 in PBS solution, to improve the assay sensitivity by reducing background interference. The coverslips were picked up, allowed to dry for 2 h, turned over and permanently

mounted to the glass slide using one drop of Vectashield™ HardSet™ Mounting Medium with DAPI (refractive index 1.452).

Analysis of the control and treated L929 cells was performed using a Leica™ TCS SP5 confocal laser scanning microscope equipped with a 405 nm diode UV laser for blue fluorescent labeling (DAPI filter set, *Ex*: 405 nm, *Em*: 461 nm), an argon laser for green labeling (Green Fluorescent Protein filter set, *Ex*: 488 nm, *Em*: 525 nm) and DPSS 561 laser for red fluorescent labeling (Alexa filter set, *Ex*: 581 nm, *Em*: 609 nm). The scan speed was 400 Hz. The used objective was a Leica™ HCX PL APO 63x magnification/1.3 numerical aperture objective lens embedded in 100% glycerol (refractive index 1.46). Images were taken at 1024 pixel × 1024 pixel resolution. The photomultiplier gain and offset configurations were set up on control cells so as to correct the images for green auto-fluorescence. A *Z*-stack of 50 frames covering a depth of 10 μm was recorded for assessment of the NP distribution across the section. The images were processed using the ImageJ (Image Processing and Analysis in Java) and ICY (an open community platform for bioimage informatics) software.

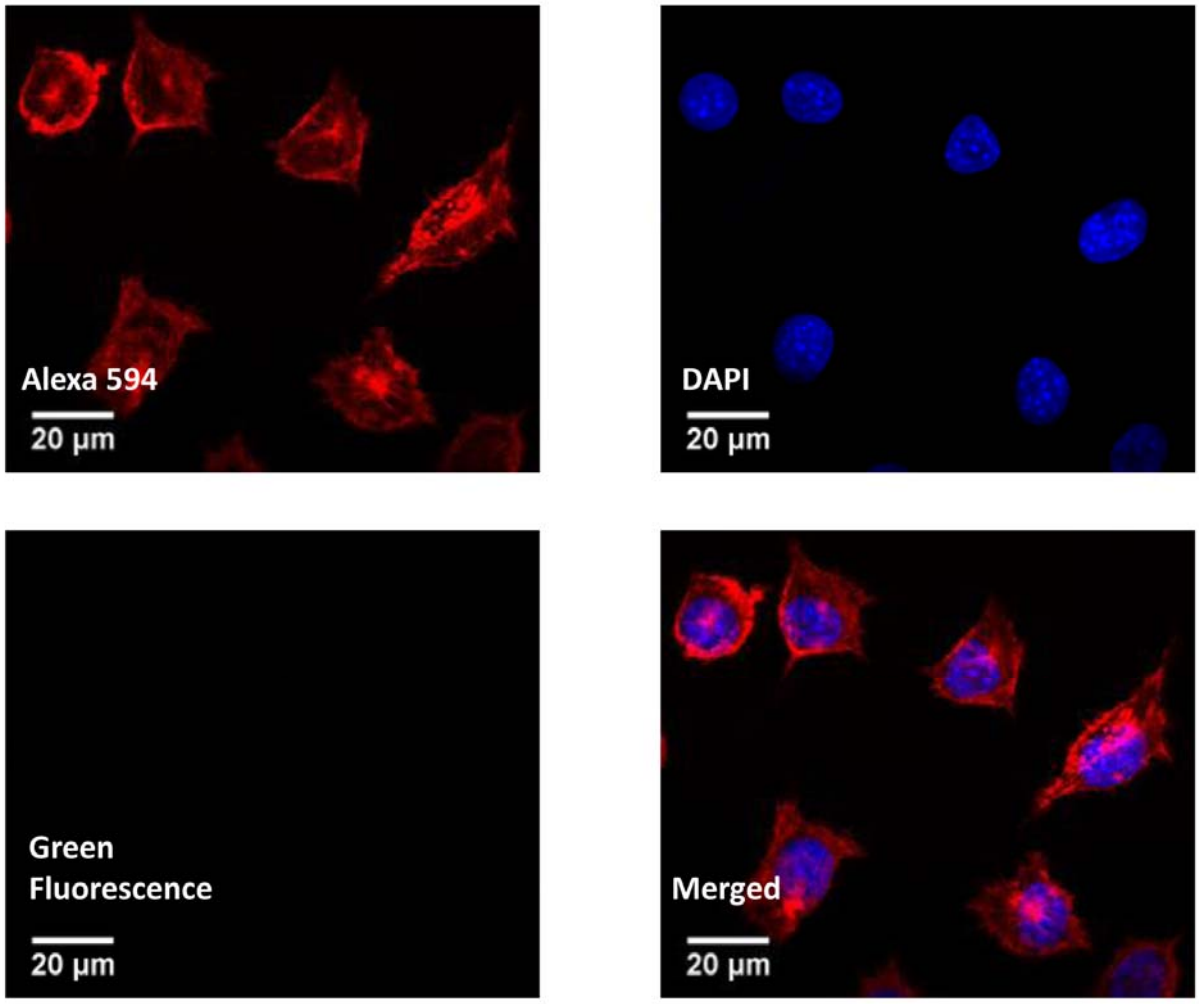

Figure SI-12. Confocal laser scanning microscopy images for L929 cells untreated with PIC micelles, after 24 h of incubation. The corresponding images for the cells treated with PIC micelles are provided as Figure 4 in the article.

References for Supporting Information

(1) Lin, M.; Xu, P.; Zhong, W., Preparation, Characterization, and Release Behavior of Aspirin-Loaded Poly(2-hydroxyethyl acrylate)/Silica Hydrogels. *Journal of Biomedical Materials Research, Part B: Applied Biomaterials* **2012,** *100B* (4), 1114-1120.

(2) Davis, K. A.; Matyjaszewski, K., Atom Transfer Radical Polymerization of tert-Butyl Acrylate and Preparation of Block Copolymers. *Macromolecules* **2000,** *33* (11), 4039-4047.

(3) Mühlebach, A.; Gaynor, S. G.; Matyjaszewski, K., Synthesis of Amphiphilic Block Copolymers by Atom Transfer Radical Polymerization (ATRP). *Macromolecules* **1998,** *31* (18), 6046-6052.

(4) Sjöback, R.; Nygren, J.; Kubista, M., Absorption and Fluorescence Properties of Fluorescein. *Spectrochimica Acta Part A: Molecular and Biomolecular Spectroscopy* **1995,** *51* (6), L7-L21.

(5) Margulies, D.; Melman, G.; Shanzer, A., Fluorescein as a Model Molecular Calculator with Reset Capability. *Nature Materials* **2005,** *4* (10), 768-771.

(6) Hungerford, G.; Benesch, J.; Mano, J. F.; Reis, R. L., Effect of the Labelling Ratio on the Photophysics of Fluorescein Isothiocyanate (FITC) Conjugated to Bovine Serum Albumin. *Photochemical & Photobiological Sciences* **2007,** *6* (2), 152-158.

(7) Schaefer, D. W.; Han, C. C., Quasielastic Light Scattering from Dilute and Semidilute Polymer Solutions. In *Dynamic Light Scattering: Applications of Photon Correlation Spectroscopy*, Pecora, R., Ed. Springer US: Boston, MA, 1985; pp 181-243.

(8) LifeTechnologies™, L929 Cells. Cell Line database: LifeTechnologies: 2014; Vol. Technical resources/Cell Lines/L/L929 Cells.